sponding to a particular value of ϵ. For each graph the resonator cross-sectional dimensions are given. Radius A of the cylindrical resonator is given explicitly; widths A^* and B^* of the rectangular resonator must be calculated from the given value of β [using (6)]. Alternatively A^* and B^* may be obtained graphically with the aid of Fig. 9. This is a graph of A^* vs. B^* for parametric values of β. The results shown in Figs. 3–8 cover a range of frequencies from zero to 30 kMc/s lengths from zero to 30 mils (1 mil $= 10^{-3}$ inch), ϵ from 50 to 500, A from 25 to 200 mils, and β from 0.01202 to 0.09619 mils^{-1}. This range of β includes cross-sectional widths from 40 to 600 mils. The actual program included a much larger range of values. The complete results will be presented in graphical and tabular form in an AFCRL Research Report [9]. The values given here hopefully include those of most practical interest in the microwave region at the present time.

References

[1] R. D. Richtmyer, "Dielectric resonator," *J. Appl. Phys.*, vol. 10, p. 391, June 1939.
[2] A. Okaya, "The rutile microwave resonators," *Proc. IRE*, vol. 48, p. 1921, November 1960.
[3] R. O. Bell and G. Rupprecht, "Measurement of small dielectric losses in material with a large dielectric constant at microwave frequencies," *IRE Trans. on Microwave Theory and Techniques*, vol. 9, pp. 239–242, May 1961.
[4] A. Okaya and L. F. Barash, "The dielectric microwave resonator," *Proc. IRE*, vol. 50, p. 2081, October 1962.
[5] H-Y. Yee, "An investigation of microwave dielectric resonators," Hansen Labs., Stanford Univ., Stanford, Calif., M. L. Rept. 1065, July 1963.
[6] H. J. Shaw, et al., "Attenuation of hypersonic waves in sapphire and rutile at 2.8 Gc/sec and room temperature," *Appl. Phys. Letters*, vol. 4, no. 2, p. 28, January 15, 1964.
[7] G. L. Vick and L. E. Hollander, "Ultrasonic measurement of the elastic moduli of rutile," *J. Acoust. Soc. Amer.*, vol. 32, no. 8, p. 947, August 1960.
[8] M. Stiglitz and J. C. Sethares, "Frequency stability in dielectric resonators," *Proc. IEEE*, vol. 53, pp. 311–312, March 1965.
[9] S. J. Naumann and J. C. Sethares, Research Rept. AFCRI, 65-867, Physical Sciences Research Papers No. 173, November 1965.
[10] W. Gerbes, Private communication

Impedances of Offset Parallel-Coupled Strip Transmission Lines

J. PAUL SHELTON, JR., MEMBER, IEEE

Abstract—**An offset parallel-coupled strip configuration is described, in which the mechanical parameters are strip width, strip offset, and ratio of strip spacing to ground-plane spacing. The electrical parameters are dielectric constant, characteristic impedance, even and odd mode impedance. The configuration is analyzed by conformal mapping techniques. Explicit design equations are derived in which the mechanical parameters are expressed in terms of the electrical parameters. Illustrative results are presented, and the limitations on coupling strength, characteristic impedance, and strip configuration are discussed.**

Introduction

MANY MICROWAVE components are based upon parallel-coupled transmission-line sections. Examples are found among directional couplers, baluns, hybrid junctions, phase shifters, and filters [1]–[3]. In some cases, several coupled regions are used to obtain increased control over the theoretical characteristics of the component. In general, multisection components require different coupling values for the various sections. The subject of this paper is the analysis of a parallel-coupled strip transmission-line configuration that permits smooth variation of coupling from some designed maximum level to any lower value.

The first strip transmission-line technique for realizing variable coupling was edge-coupled coplanar strips [4]. The drawback to this method is the limitation of ρ, the ratio of even to odd mode impedance, to a maximum of two or three.

Getsinger proposed a technique for achieving very tight coupling in which a line with single center strip is sandwiched between the two strips of a second line [5]. This method requires the use of four layers of dielectric, and the transmission lines are unlike, one having single strip and one having double strips. Furthermore, it is somewhat difficult to determine the maximum coupling that is available for a given strip spacing.

Impedance relations for parallel strips, one above the other between ground planes, were derived by Cohn [6]. This configuration requires three dielectric layers and provides maximum coupling for given layer thicknesses. For this configuration, variation in coupling can be easily achieved in practice by offsetting the strips without changing the thicknesses of the dielectric layers. In general, both strip width and overlap are functions of

Manuscript received March 25, 1965; revised August 25, 1965.
The author is with the Institute for Defense Analyses, Arlington, Va. He was formerly with Radiation Systems, Inc., Alexandria, Va.

coupling. This offset configuration has not previously been available to the microwave engineer because it has not been analyzed. An analysis is presented here.

In the following paragraphs, the even and odd mode impedances are derived for the offset configuration shown in Fig. 1, in which zero-thickness strips are located in the dielectric-filled region between infinite ground planes. First, expressions for the necessary fringing capacitances are obtained. Then the equations for the various impedances are derived. Finally, curves of coupling vs. strip width and offset are presented for sample configurations. The derivation of fringing capacitance is described in the Appendix.

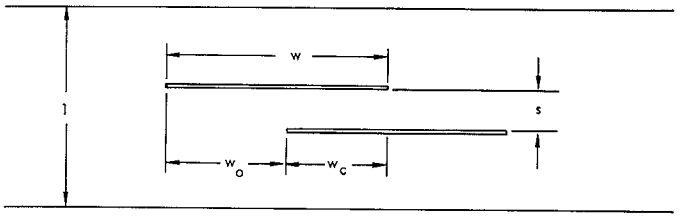

Fig. 1. Offset parallel-coupled strip transmission lines.

It will be noted that the uncoupled single strip, which is obtained when the separation is made very large, is not centered between the ground planes. This configuration has been avoided by some workers in the field because of concern over parallel-plate radiation. This concern is unfounded. The same care must be taken with any unbounded transmission line to avoid radiation, whether it uses a centered strip, an off-center strip, or an open strip over single ground plane. The configuration described in this paper has been used successfully over three years by the author and his associates.

Fringing Capacitances

The technique used to determine even and odd mode impedance is an approximate one. That is, the capacitance between strip and ground is separated into parallel-plate and fringing components. As a result, there are two cases to be considered, depending on the relative positions of the strip edges. In Fig. 2(a), the case for tight coupling is shown, and the approximate limitations on strip dimensions are

$$\frac{w}{1-s} \geqq 0.35$$

$$\frac{w_c}{s} \geqq 0.7.$$

For loose coupling, shown in Fig. 2(b), the limitations are

$$\frac{w}{1-s} \geqq 0.35$$

$$\frac{2w_o}{1+s} \geqq 0.85.$$

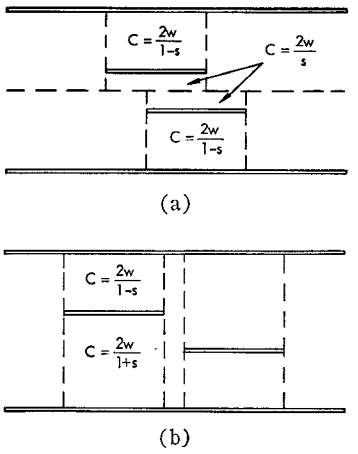

Fig. 2. Coupling configurations. (a) Configuration for tight coupling. (b) Configuration for loose coupling.

The effects of these limitations on the allowable range of strip configuration, maximum coupling, and characteristic impedance are discussed in a later section.

The derivation of the fringing capacitances is discussed in the Appendix. The Schwartz-Cristofel transformation is used to achieve the following results:

Tight coupling:

$$\pi C_{fo} = -\frac{2}{1-s}\log s + \frac{1}{s}\log\left[\frac{pr}{(p+s)(p+1)(r-s)(1-r)}\right] \quad (1)$$

$$\pi C_{fe} = -\frac{2s}{1-s}\log s - 2\log s + 4\log(s+pr) - \log pr(p+s)(p+1)(r-s)(1-r) \quad (2)$$

where

$$r = \frac{p + \frac{1+s}{2}}{1 + p\left(\frac{1+s}{2s}\right)} \qquad (o < p < \infty).$$

Loose coupling:

$$\pi C_{fo} = \frac{2}{1+s}\log\left(\frac{1+a}{a(1-q)}\right) - \frac{2}{1-s}\log q \quad (3)$$

$$\pi C_{fe} = \frac{2}{1+s}\log\left[\frac{1+a}{a(1-q)}\right] - \frac{2}{1-s}\log q - 2\log\left(\frac{1+aq}{aq}\right) \quad (4)$$

where

$$q = \left(\frac{s+1}{2}\right)\left\{\frac{a + \frac{2s}{s+1}}{a + \frac{s+1}{2}}\right\}.$$

Furthermore, the conformal mapping procedure yields the following expressions for offset dimensions:

For tight coupling,

$$\pi w_o = \frac{1+s}{2}\log\frac{p}{r} + \frac{1-s}{2}\log\left(\frac{1+p}{s+p}\right)\left(\frac{r-s}{1-r}\right). \tag{5}$$

For loose coupling,

$$\pi w_c = s\log\frac{q}{a} + (1-s)\log\left(\frac{1-q}{1+a}\right). \tag{6}$$

Impedance Equations

Although it is possible to plot families of curves relating C_{fo}, C_{fe}, w, w_c, and s, it is very useful to relate the fringing and parallel-plate capacitances and the associated strip dimensions to the even and odd mode impedances, which are the basic design parameters of any component in which the coupled lines are used. One listing of parameters, which can be considered the independent variables, is

Z_o, the characteristic impedance

ϵ_r, the relative dielectric constant of the medium

ρ, the ratio of Z_{oe} to Z_{oo}.

The basic relationships are

$$\begin{aligned} Z_{oe} &= \sqrt{\rho}\, Z_o \\ Z_{oo} &= Z_o/\sqrt{\rho} \\ C_e &= 120\pi/\sqrt{\epsilon_r}\, Z_{oe} \\ C_o &= 120\pi/\sqrt{\epsilon_r}\, Z_{oo}. \end{aligned} \tag{7}$$

For tight coupling, the mode capacitances may be expressed

$$\begin{aligned} C_o &= 2w\left(\frac{1}{1-s}+\frac{1}{s}\right) + C_{fo} \\ &= \frac{2w}{s(1-s)} + C_{fo} \\ C_e &= \frac{2w}{1-s} + C_{fe} \end{aligned} \tag{8}$$

where C_{fo} and C_{fe} are given by (1) and (2), and the parallel-plate capacitances are those indicated in Fig. 2(a). Note that the capacitance between strips is approximated by $2w/s$ rather than $2w_c/s$, an artifice which simplifies the expressions for fringing capacitances and allows explicit solution.

For loose coupling, the capacitances are

$$\begin{aligned} C_o &= 2w\left(\frac{1}{1-s}+\frac{1}{1+s}\right) + C_{fo} - C_f(a=\infty) \\ &= \frac{4w}{1-s^2} + C_{fo} + C_f(a=\infty) \\ C_e &= \frac{4w}{1-s^2} + C_{fe} + C_f(a=\infty) \end{aligned} \tag{9}$$

where C_{fo} and C_{fe} are given by (3) and (4), and $C_f(a=\infty)$ is the fringing capacitance at the edge of a single, uncoupled strip. The parallel-plate capacitances are those indicated in Fig. 2(b). It is easily found that

$$\pi C_f(a=\infty) = -\frac{2}{1+s}\log\left(\frac{1-s}{2}\right) - \frac{2}{1-s}\log\left(\frac{1+s}{2}\right). \tag{10}$$

At this point, the continuity of the development is strengthened if the cases are treated separately. It is noted that the equations so far obtained do not even present an implicit solution to the problem. It is necessary to find some connection between the results of the conformal mapping and the basic relationships of (7)–(9).

Derivation for Tight Coupling

For tight coupling, the required connection results from

$$\begin{aligned} C_e - s\,C_o &= C_{fe} - s\,C_{fo} && \text{[from (8)]} \\ &= \frac{2}{\pi}\log\left[\frac{\left(1+\frac{pr}{s}\right)^2}{\left(\frac{pr}{s}\right)}\right] && \text{[from (1) and (2)]} \\ &= \left(\frac{1-\rho s}{\sqrt{\rho}}\right)\frac{120\pi}{\sqrt{\epsilon_r}\, Z_o} && \text{[from (7)]} \end{aligned}$$

Therefore, the implicit solution for tight coupling is

$$\frac{1-\rho s}{\sqrt{\rho}} = \frac{\sqrt{\epsilon_r}\, Z_o}{60\pi^2}\log\left[\frac{\left(1+\frac{pr}{s}\right)^2}{\left(\frac{pr}{s}\right)}\right].$$

It is possible to eliminate p and r as follows:

$$\text{Let } A = \frac{(1+pr/s)^2}{(pr/s)} = \exp\left[\frac{60\pi^2}{\sqrt{\epsilon_r}\, Z_o}\left(\frac{1-\rho s}{\sqrt{\rho}}\right)\right] \tag{11}$$

$$\text{Let } B = \frac{pr}{s} = \frac{A-2\pm\sqrt{A^2-4A}}{2}. \tag{12}$$

The two signs of the square root represent the plus or minus values of w_o which produce the same value of $C_e - sC_o$. Using the equation for r in terms of p, p is found to be

$$p = \frac{(B-1)\left(\frac{1+s}{2}\right) + \sqrt{\left(\frac{1+s}{2}\right)^2 (B-1)^2 + 4sB}}{2} \tag{13}$$

where the plus sign on the root gives $p > o$.

The steps in the explicit solution, given Z_o, ϵ_r, ρ, and s, are now complete. The procedure is to solve (11) for A, (12) for B, (13) for p and r, then use (1) or (2) for C_{fo} or C_{fe}, (7) and (8) for w, and, finally, (5) for w_o.

It is worthwhile making a comparison with the results of Cohn for parallel-coupled strips. Examination of (5) reveals that $w_o = 0$ for $p = r = \sqrt{s}$. For this condition, (1) and (2) reduce to

$$C_{fo} = -\frac{2}{\pi}\left[\frac{1}{1-s}\log s + \frac{1}{s}\log(1-s)\right]$$

$$C_{fe} = -\frac{2}{\pi}\left[\frac{s}{1-s}\log s + \log(1-s) - \log 4\right],$$

which are equivalent to Cohn's approximate results, as given in his equations (4), (5), (6), and (7) [6]. Furthermore, the implicit solution reduces to

$$\frac{1 - \rho_{\max} s}{\sqrt{\rho_{\max}}} = \frac{\sqrt{\epsilon_r}\, Z_o}{60\pi^2}\log 4. \tag{14}$$

Equation (14) is extremely useful. It relates $\rho_{\max}$, s, ϵ_r, and Z_o in a single expression and allows direct solution of the zero-offset configuration. In many practical cases, one has a maximum value of ρ to be realized; (14) specifies the required corresponding value of s. It is emphasized, however, that (14) is limited by the approximate analysis used. For very large $\rho_{\max}$ or small s, one must use Cohn's virtually exact equations, (1), (2), and (3) [6]. In general, (14) holds for

$$\frac{\sqrt{\rho_{\max}\epsilon_r}\, Z_o}{60\pi^2}\log 4 < 0.5,$$

provided $\rho_{\max} > 2$.

Derivation for Loose Coupling

For loose coupling, the required combination of expressions is

$$\Delta C = C_o - C_e = \frac{120\pi}{\sqrt{\epsilon_r}\, Z_o}\left(\frac{1+\rho}{\sqrt{\rho}}\right) \qquad \text{[from (8)]}$$

$$= \frac{2}{\pi}\log\left(\frac{1+aq}{aq}\right). \qquad \text{[from (3) and (4)]}$$

Letting

$$k = aq,$$

$$\Delta C = \frac{2}{\pi}\log\left(\frac{1+k}{k}\right)$$

or

$$k = \frac{1}{\exp\left(\frac{\pi\Delta C}{2}\right) - 1}. \tag{15}$$

Using the equation for q in terms of a, then solving for a in terms of k,

$$a = +\sqrt{\left(\frac{s-k}{s+1}\right)^2 + k} - \frac{s-k}{s+1}.$$

The positive root guarantees $a > 0$.

The explicit solution for loose coupling, given Z_o, ϵ_r, ρ, and s, is now accomplished by solving (8) for ΔC, (15) for k, (16) for a and q, (3) or (4) for C_{fo} and C_{fe}, (9) for w, and (6) for w_C.

Collected Equations

An orderly arrangement of the design equations resulting from the previous section is presented in order to facilitate the computation of parameters.

Equations for tight coupling:

$$A = \exp\left[\frac{60\pi^2}{\sqrt{\epsilon_r}\, Z_o}\left(\frac{1-\rho s}{\sqrt{\rho}}\right)\right]$$

$$B = \frac{pr}{s} = \frac{A - 2 + \sqrt{A^2 - 4A}}{2}$$

$$p = \frac{(B-1)\left(\frac{1+s}{2}\right) + \sqrt{\left(\frac{1+s}{2}\right)^2 (B-1)^2 + 4sB}}{2}$$

$$r = \frac{sB}{p}\left[\text{also, } r = \frac{p + \frac{1+s}{2}}{1 + p\left(\frac{1+s}{2s}\right)}, \quad o < p < \infty\right]$$

$$C_{fo} = \frac{1}{\pi}\left\{-\frac{2}{1-s}\log s + \frac{1}{s}\log\left[\frac{pr}{(p+s)(1+p)(r-s)(1-r)}\right]\right\}$$

$$C_o = \frac{120\pi\sqrt{\rho}}{\sqrt{\epsilon_r}\, Z_o}$$

$$w = \frac{s(1-s)}{2}(C_o - C_{fo})$$

$$w_o = \frac{1}{2\pi}\left[(1+s)\log\frac{p}{r} + (1-s)\log\left(\frac{1+p}{s+p}\right)\left(\frac{r-s}{1-r}\right)\right].$$

The condition for tightest coupling $w_o = 0$ is given by

$$\frac{1 - \rho_{\max} s}{\sqrt{\rho_{\max}}} = \frac{\sqrt{\epsilon_r}\, Z_o}{60\pi^2}\log 4.$$

Equations for loose coupling:

$$C_o = \frac{120\pi\sqrt{\rho}}{\sqrt{\epsilon_r}\,Z_o}$$

$$\Delta C = \frac{120\pi}{\sqrt{\epsilon_r}\,Z_o}\,\frac{\rho - 1}{\sqrt{\rho}}$$

$$k = \frac{1}{\exp\dfrac{\pi\Delta C}{2} - 1}$$

$$a = +\sqrt{\left(\frac{s-k}{s+1}\right)^2 + k} - \frac{s-k}{s+1}$$

$$q = \frac{k}{a}\left[\text{or } q = \left(\frac{s+1}{2}\right)\left(\frac{a + \dfrac{2s}{s+1}}{a + \dfrac{s+1}{2}}\right)\right]$$

$$C_{fo} = \frac{2}{\pi}\left[\frac{1}{1+s}\log\frac{1+a}{a(1-q)} - \frac{1}{1-s}\log q\right]$$

$$w_c = \frac{1}{\pi}\left[s\log\frac{q}{a} + (1-s)\log\left(\frac{1-q}{1+a}\right)\right]$$

$$C_f(a=\infty) = -\frac{2}{\pi}\left[\frac{1}{1+s}\log\left(\frac{1-s}{2}\right) + \frac{1}{1-s}\log\left(\frac{1+s}{2}\right)\right]$$

$$w = \frac{1-s^2}{4}\left[C_o - C_{fo} - C_f(a=\infty)\right].$$

Illustrative Results and Limitations on Parameters

In the particular application for which the coupled impedances were evaluated, two of the parameters of (14) were held fixed. The dielectric constant ϵ_r was 2.32, corresponding to polyolefin materials, and the characteristic impedance was 50 ohms. It is conceivable that many similar situations, in which the operating impedance and the dielectric material are predetermined, might be encountered. In such a case, the remaining parameters s and $\rho_{\max}$ can be related by a curve, as shown in Fig. 3. The value of $\rho_{\max}$ varies from two to six, and the approximate range of s is 0.1 to 0.4, accounting for the probable range of coupling values amenable to this strip configuration.

Also shown on the curve are the values of s which correspond to layer thickness ratios involving small integral numbers. These values are more easily realized in terms of readily available sheet thicknesses, although it must be noted that material manufacturers are developing considerable flexibility in this respect.

Since the fringing capacitances were determined by an approximate procedure and the accuracy of the results was based on maintaining certain limitations on the strip dimensions, it is of interest to estimate the effects of these limitations on the allowable physical and electrical parameters of the coupled strip configuration. The following limitations were imposed by the fringing capacitance calculation:

In general:

$$\frac{w}{1-s} \geqq 0.35.$$

For loose coupling:

$$\frac{2w_o}{1+s} \geqq 0.85.$$

For tight coupling:

$$\frac{w_c}{s} \geqq 0.7.$$

The first inequality concerns the parallel-plate region between the outer surface of the strip and the ground plane. The second expression deals with the region between the "exposed" inner strip surface and the opposite ground plane; the constant chosen for this condition is 0.85 rather than 0.7 because the fringing fields from the edge of the intervening strip extend into this region. The third relation defines the parallel-plate region between strips.

The effects on strip spacing s and on $\sqrt{\epsilon_r}Z_o$ are considered in Fig. 4. Curve A is the limit imposed by the relationship $2w/(1+s) \geqq 0.7$ for a single uncoupled strip. Curve B is obtained when the strips are located one over the other ($w_o = 0$), and the limitation $w/s \geqq 0.7$ is applied. Thus, curves A and B define the allowable parameters for parallel coupled strips when offsetting is not used. Curve C is obtained by setting $w_c/s = 0.7$ and $2w_o/(1+s) = 0.85$, then assuming $w = w_o + w_c$ for the uncoupled strip and calculating the corresponding value of $\sqrt{\epsilon_r}Z_o$. Since the width of coupled strips is always smaller than that of uncoupled strips, curve C is too high. Two calculated points are available which satisfy the criteria of curve C, and they are shown on the dashed curve. The dashed curve is a rough estimate of the correct location of curve C. The shaded region represents the range of parameters for which the strip dimensions for all values of coupling are very accurately obtained. That is, the curves based on tight- and loose-coupling approximation can be joined by a negligible discontinuity.

The results of Fig. 4 should not be interpreted to forbid the use of parameters falling outside of the shaded region. In some cases, the coupling values which correspond to inaccurate strip dimensions are not used. In other cases, the inaccurate portions of the curves can be corrected by interpolation. However, it is seen that the most versatile application of this design procedure is obtained for values of s in the range of approximately 0.14 to 0.20, corresponding to values of $\rho_{\max}$ in the neighborhood of 3.5 to 4.5.

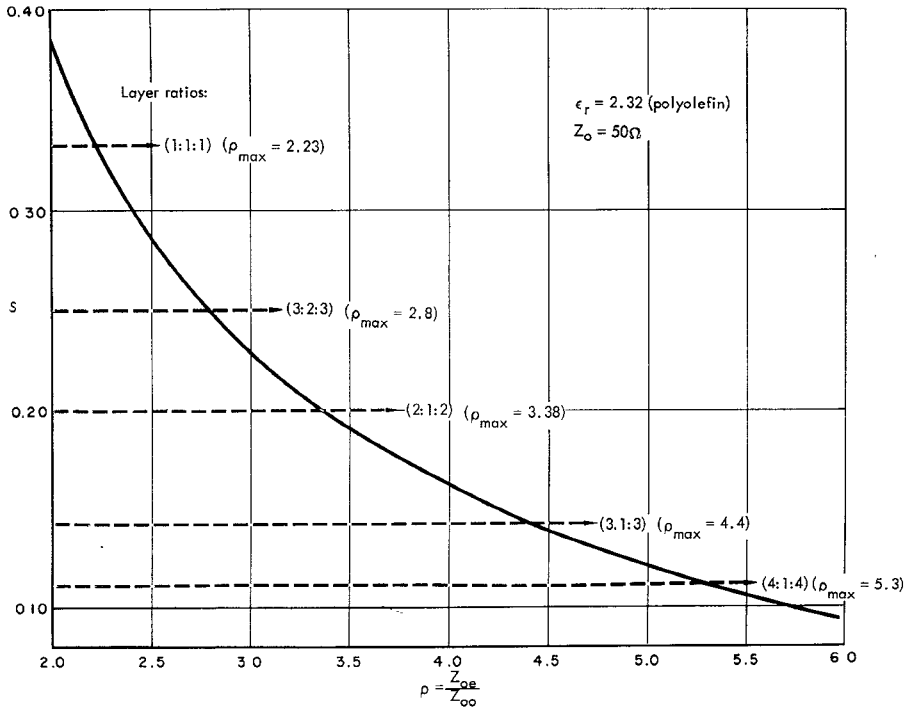

Fig. 3. Relationship between s and ρ.

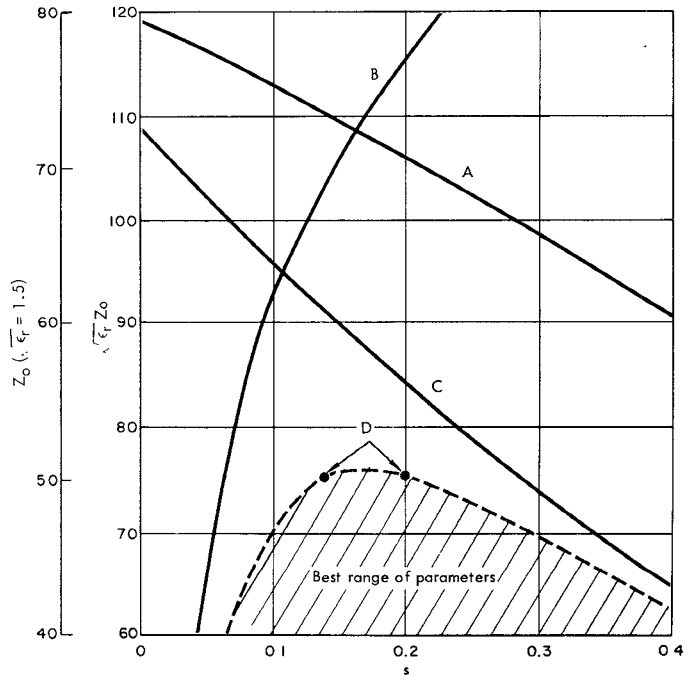

A $\frac{2w}{1+s}$ > .7 for single uncoupled strip

B $\frac{w}{s}$ > .7 for parallel strips, maximum coupling

C $\frac{w_c}{s}$ > .7, $\frac{2w_o}{1+s}$ > .85 for offset strips; approximate

D Computed points for $\frac{w_c}{s}$ > .7, $\frac{2w_o}{1+s}$ > .85

Fig. 4. Limitation on parameters, s and $\sqrt{\epsilon_r} Z_0$.

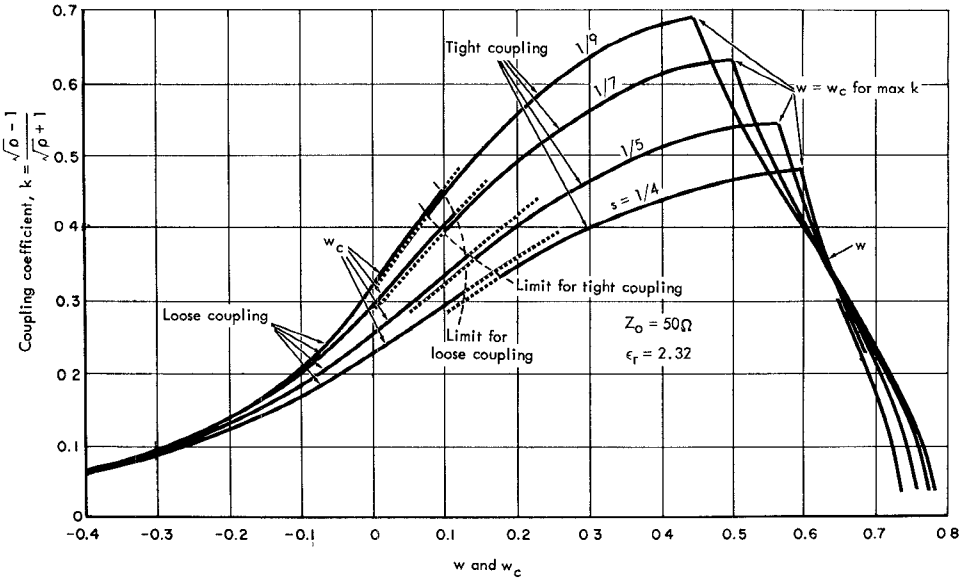

Fig. 5. Representative coupling curves.

Figure 5 contains curves relating coupling coefficient

$$k = \frac{\sqrt{\rho} - 1}{\sqrt{\rho} + 1}$$

to strip dimensions for representative values of s, for $Z_o = 50\Omega$ and $\epsilon_r = 2.32$. An indication of the approximation involved in the analysis is seen in the imperfect match of the strong- and weak-coupling curves.

Conclusions

A design procedure for offset parallel-coupled strips has been derived. The equations are arranged in terms of the electrical parameters, coupling strength (ρ) and characteristic impedance (Z_o). Because of the approximations involved in the conformal mapping analysis, limitations are imposed on the range of characteristic impedance that can be used and on the ratio of strip separation to ground-plane spacing(s). However, the ranges in which good accuracy is achieved are those most likely to be used in practical strip transmission-line components and circuits.

Appendix

Derivation of Fringing Capacitances

The procedure for determining the fringing capacitances for a strip transmission-line configuration is straightforward and is outlined for review purposes. The term "fringing" is generally used when the fields at one edge of the strip do not significantly influence those at the opposite edge. Thus, the strips can be assumed to be infinitely wide, as indicated in Fig. 6. The fringing capacitance is defined as the difference between the ideal parallel-plate capacitance and the actual value. For infinite strips, of course, the capacitances become infinite, but the difference is finite.

The steps in the procedure are as follows:

1) The conductor configuration of Fig. 6 is mapped onto the real axis of the complex plane by means of the Schwartz-Cristofel transformation. In the cases under consideration, the transformation is particularly simple. For both configurations considered, the polygon in the w-plane being mapped onto a real axis of the z-plane has six sides, and the vertex angles are all ± 180 degrees. One result of this condition is that the differential equation of the transformation is readily soluble in terms of logarithmic functions.
2) The parallel-plate capacitances for even and odd modes are selected, and the appropriate expressions are written.
3) The actual capacitances are determined by calculating charge density for unit voltages on the strips. The result is in the form of capacitance distribution.
4) The fringing capacitance is obtained by subtracting the expression of Step 2 from that of Step 3 and integrating over the infinite strip cross section.

If the reader is unfamiliar with this procedure, an excellent description and illustrative example has recently been presented by Wheeler [7].

Case for Large ρ: Considering first the case for strong coupling or large ρ, the conformal transformation is shown in Fig. 7. The equation of the transformation is

$$w = \frac{1}{\pi}\left[s \log z + \frac{1 - s}{2} \log (z - 1)\left(z + \frac{pr}{s}\right)\right]$$

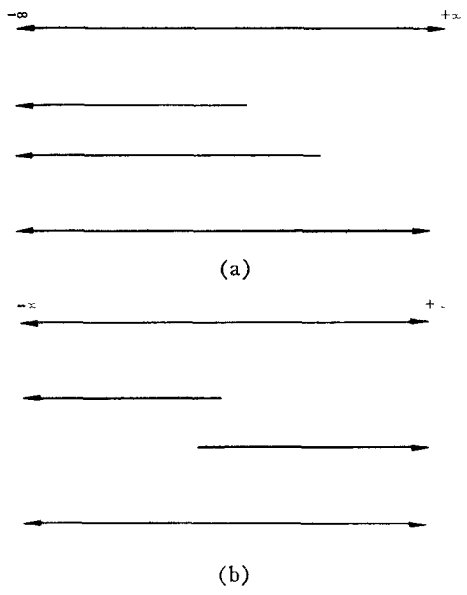

Fig. 6. Infinite strip approximation. (a) Strong coupling. (b) Loose coupling.

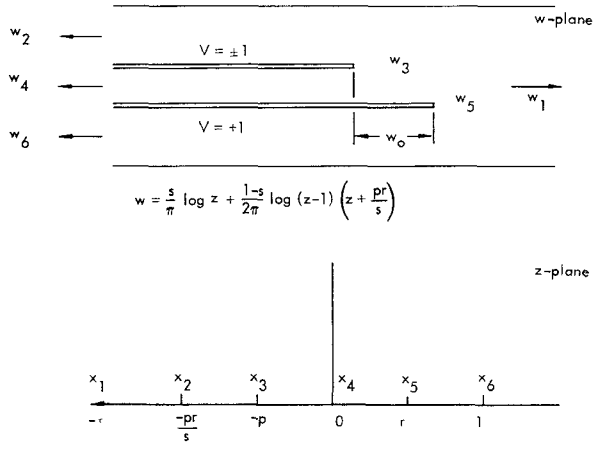

Fig. 7. Conformal transformation—large ρ.

where

$$r = \frac{p + \dfrac{1+s}{2}}{1 + p\left(\dfrac{1+s}{2s}\right)} \qquad \begin{matrix} 0 < p < \infty \\ \dfrac{2s}{1+s} < r < \dfrac{1+s}{2} \end{matrix}.$$

It is immediately possible to express the offset width w_o, in terms of s, p, and r,

$$w_o = \frac{1}{\pi}\left[\frac{1+s}{2}\log\frac{p}{r} + \frac{1-s}{2}\log\left(\frac{1+p}{s+p}\right)\left(\frac{r-s}{1-r}\right)\right].$$

The basis for the parallel-plate capacitances is indicated in Fig. 8. For the even mode, $C_{pe} = C_1 + C_2$; for the odd mode, $C_{po} = C_1 + C_2 + C_3 + C_4$. The capacitance of both strips to ground is computed for this case because the strip arrangement is not symmetrical. The resulting

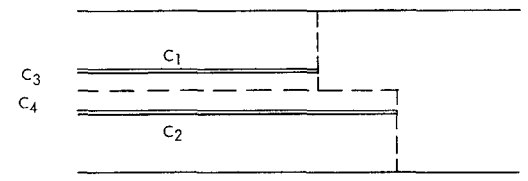

Fig. 8. Parallel-plate capacitances—large ρ.

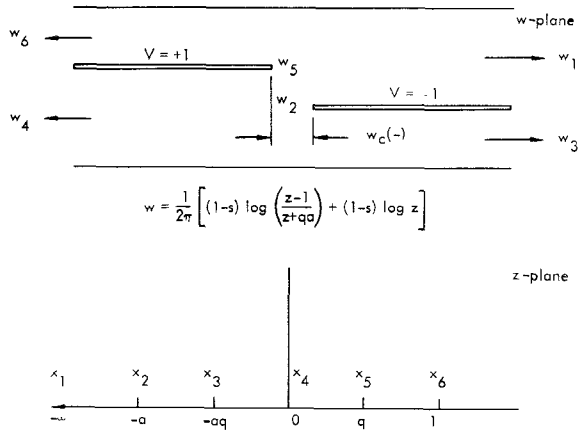

Fig. 9. Conformal transformation—small ρ.

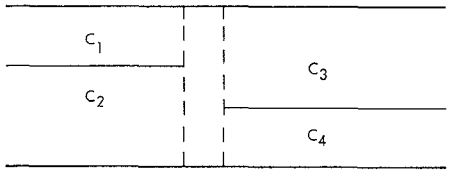

Fig. 10. Parallel-plate capacitances—small ρ.

fringe capacitance is equal to the sum of the fringe capacitances of both edges of a single strip of finite width. Application of the previously mentioned conventional techniques yields the required results for the fringing capacitances.

Case for Small ρ: The conformal transformation for the loose coupling configuration is shown in Fig. 9. The equation of the transformation is

$$w = \frac{1}{2\pi}\left[(1-s)\log\left(\frac{z-1}{z+qa}\right) + (1+s)\log z\right]$$

where

$$q = \frac{s+1}{2}\left|\frac{a + \dfrac{2s}{s+1}}{a + \dfrac{s+1}{2}}\right| \qquad \begin{matrix} 0 < a < \infty \\ \dfrac{2s}{s+1} < q < \dfrac{s+1}{2} \end{matrix}.$$

As for the strong coupling case, it is possible to determine w_c directly:

$$w_c = \frac{1}{\pi}\left[s\log\left(\frac{q}{a}\right) + (1-s)\log\left(\frac{1-q}{1+a}\right)\right].$$

A negative value of w_c represents a gap rather than overlap between strip edges.

The basis for parallel-plate capacitance is shown in Fig. 10. For both even and odd modes, $C_p = C_1 + C_2$. Since the strip arrangement is symmetrical in this case, the fringe capacitance is calculated for only one strip. Again, the required expressions for fringing capacitance are found by conventional methods.

Acknowledgment

J. Mosko of Naval Ordnance Test Station, China Lake, Calif., has programmed the design equations for electronic computation. He supplied the data from which Fig. 5 was prepared. He can provide a copy of the Fortran program to anyone who wishes to use it.

References

[1] E. M. T. Jones and J. T. Bolljahn, "Coupled-strip-line filters and directional couplers," *IRE Trans. on Microwave Theory and Techniques*, vol. MTT-4, pp. 75–81, April 1956.

[2] J. K. Shimizu and E. M. T. Jones, "Coupled-transmission-line directional couplers," *IRE Trans. on Microwave Theory and Techniques*, vol. MTT-6, pp. 403–410, October 1958.

[3] S. B. Cohn, "Direct-coupled-resonator filters," *Proc. IRE*, vol. 45, pp. 187–196, February 1957.

[4] S. B. Cohn, "Characteristic impedances of broadside-coupled strip transmission lines," *IRE Trans. on Microwave Theory and Techniques*, vol. MTT-8, pp. 633–637, November 1960.

[5] W. J. Getsinger, "A coupled strip-line configuration using printed-circuit construction that allows very close coupling," *IRE Trans. on Microwave Theory and Techniques*, vol. MTT-9, pp. 535–544, November 1961.

[6] S. B. Cohn, "Shielded coupled-strip transmission line," *IRE Trans. on Microwave Theory and Techniques*, vol. MTT-3, pp. 29–38, October 1955.

[7] H. A. Wheeler, "Transmission-line properties of parallel wide strips by a conformal-mapping approximation," *IEEE Trans. on Microwave Theory and Techniques*, vol. MTT-12, pp. 280–289, May 1964.

Theoretical Analysis of Twin-Slab Phase Shifters in Rectangular Waveguide

ERNST SCHLÖMANN

Abstract—**The differential phase shift and the losses to be expected in phase shifters using two oppositely magnetized ferrite slabs located symmetrically in a rectangular waveguide have been calculated for various locations and thicknesses of the ferrite slabs. For small thicknesses of the ferrite slabs, the differential phase shift increases rapidly with increasing thickness reaching a maximum when the thickness is approximately 1/10 of the free space wavelength. The calculated insertion loss of a 360-degree phase shifter decreases with increasing slab thickness for small thickness, reaching a minimum when the thickness is approximately 1/25 of the free space wavelength. The minimum insertion loss calculated with the assumption that the imaginary part of the diagonal component of the permeability tensor is 0.01 and that dielectric loss can be neglected is approximately 0.85 dB. The peak power handling capability has also been analyzed. It can conveniently be summarized in terms of a high-power figure of merit. For reasonably high values of this figure of merit, a peak power capability of the order of 100 kW is anticipated.**

I. Introduction

ONE OF THE more promising device configurations for digital ferrite phase shifters is that of a rectangular waveguide containing circumferentially magnetized ferrite toroids of suitable length [1], [2]. Such a structure is shown in Fig. 1. A very similar structure, which is more readily amenable to theoretical analysis, is shown in Fig. 2. Here the ferrite toroid has been replaced by two oppositely magnetized slabs which extend over the complete height of the waveguide. The propagation of electromagnetic waves through waveguides of the type shown in Fig. 2 has previously been analyzed by Lax et al. [3], [4] and by von Aulock [5]. Here we use substantially the notation of von Aulock.

In the previous work, only the differential phase shift and the field configuration have been discussed. The present paper contains more detailed results than previously published, concerning the differential phase shift and its dependence upon parameters such as spacing, width, dielectric constant, and remanent magnetization of the ferrite slabs. In addition, the present paper contains a discussion of the insertion loss and the peak power limitations of these devices.

For odd TE_{n0}-modes the characteristic equation for the reduced propagation constant Γ can be expressed as

$$\cot \delta = \frac{\nu(1 + \cot \alpha_1 \cot \alpha_2) + \zeta \cot \alpha_1 + \eta \cot \alpha_2}{\cot \alpha_1 \cot \alpha_2 - 1} \quad (1)$$

Manuscript received June 25, 1965; revised September 7, 1965. The work reported in this paper was supported by the U. S. Army Materiel Command under Contract DA 30-069-AMC-333(Y).

The author is with the Raytheon Company, Waltham, Mass.